Energy consumption of Aircraft with new propulsion systems and storage media

Yri Amandine Kambiri, Thierry Druot, Pascal Roches, Nicolas Peteilh, Nicolas Monrolin, Xavier Carbonneau

Energy consumption of aircraft with new propulsion systems and storage media

Yri Amandine Kambiri, Thierry Druot, Pascal Roches, Nicolas Peteilh, Nicolas Monrolin
Fédération ENAC ISAE-SUPAERO ONERA, Université de Toulouse, France

Xavier Carbonneau
ISAE-SUPAERO, Université de Toulouse, France.

The transition from fossil fuels to the use of sustainable energy sources is an important challenge for aviation. A particularly critical question is to identify the best mix of energies for the future air transport system. In this quest, the capability to simulate various complex scenarios, varying assumptions, models, and objectives, will play an important part. This paper provides a simple and very rapid tool to evaluate the energy consumption of parametric airplane configurations with thermal propulsion powered by kerosene, methane, hydrogen, or electric propulsion powered by hydrogen fuel cells or batteries. The maturity of the different technologies is driven by a small number of global indices that are easy to connect with state of the art or forecasts. The user can freely select the capacity, range, speed, and propulsion system of the airplane, and simulate its operations over any missions within its payload-range envelope. The tool has been validated on its capability to reproduce the characteristic weights of a range of very different aircraft, from A380 to general aviation airplanes. Finally, three use cases are presented. The first one allowed us to identify the level of technological challenge of the Alice aircraft project from EVIATION. The second one is a short mapping of the transportation potential of five different propulsion systems for the segment of 19-passenger commuter airplanes. The third use case puts the thermal hydrogen aircraft in the perspective of existing kerosene airplanes in terms of energy and structural efficiency, and reveals an optimum of the hydrogen technology.

Nomenclature

$MTOW$	=	Maximum takeoff weight
OWE	=	Operating weight empty
MWE	=	Manufacturer's weight empty
SFC	=	Specific fuel consumption (kg/s/N)
L/D	=	Lift to drag ratio
F	=	Thrust
V	=	Velocity, true airspeed
W	=	Power
E	=	Energy
$PSFC$	=	Power related specific fuel consumption
$TSFC$	=	Thrust related specific fuel consumption
ff	=	Mass fuel flow (kg/s)
fhv	=	Fuel heating value
K_r	=	Fuel reserve factor, proportion of the mission fuel for reserve
V_0	=	Airplane speed, true airspeed
V_{app}	=	Approach speed
V_{2min}	=	Minimum speed at 35ft for takeoff
V_{s1g}	=	Stall speed
n_e	=	Number of engines of the airplane
r	=	Fuel ratio
η_f	=	0.82 : Fan efficiency

g = Gravity acceleration
η = Propulsion system efficiency
η_h = Propeller efficiency $\left(\frac{F \times V}{W_{shaft}}\right)$
η_{elec} = Power efficiency of the electric motor, including its controller $\left(\frac{W_{shaft}}{W_{elec}}\right)$
η_{fcs} = Global power efficiency of the fuel cell system, including balance of plant $\left(\frac{W_{elec}}{ff \times fhv}\right)$
$M_{battery}$ = Battery mass
bed = Battery energy density
$\dot{m}$ = Airflow
gi = Gravimetric index
P_{index} = Performance index
TGI = Gravimetric index of liquid hydrogen tanks
P_i = Initial internal pressure of the tank
V_i = Internal volume of the tank
M_{tank} = Mass of the empty tank
G_{index} = Tank gravimetric index
ρ_{gas} = Gas density at P_i
η_{pw} = Power efficiency of the engine $\left(\frac{1}{psfc \times fhv} = \frac{W_{shaft}}{ff \times fhv}\right)$
η_{th} = Thermal efficiency
η_{pr} = Propulsive efficiency
$MissionFuel$ = The fuel or energy required at nominal range

I. Introduction

As any domain of activity, passenger air transport will have to drastically decrease its impact on the environment. Among all the negative effects, the contribution of air transport to radiative forcing is probably the most damaging [1, 2]. The CO_2 emissions contribute to radiative forcing, but other non-CO_2 effects of aviation are estimated to represent about 2/3 of the radiative forcing [3]. This contribution develops mainly while the aircraft is in service [4], and more specifically during cruise [5, 6]. Various studies have estimated that the carbon intensity of fossil kerosene ranges from 85 to 95 grams [7, 8] of carbon dioxide equivalent per megajoule (g CO_2e/MJ) of fuel, of which approximately 73 g CO_2e/MJ [7, 9] is due to the combustion of the fuel and the remainder to the extraction of the fuel, its processing in refineries and its transportation [10]. The five main approaches, potentially combined together, to achieve Paris Climate Agreement proposed in the literature are

1) Change the energy carrier (hydrogen, bio-sourced or synthetic methane, ammonia [11])
2) Change the way to produce fuel (bio-sourced kerosene, synthetic kerosene) [12–14]
3) Modify operations (especially during cruise to avoid contrails) [15, 16]
4) Adapt the airplane design to new practices (flight altitudes, speeds, new market segments)
5) Decrease the overall activity.

The last approach would be considered either if no alternative is found or as a consequence of the application of the other approaches. For example, a consequence of excessive demand for sustainable energy sources compared to the supply would lead to competition among the different economic sectors and competition inside the transportation sector itself. Among the other four approaches, the first and second are anticipated to bring up to 71% for the total expected gains (in terms of CO_2 emission) although the third and fourth ones would contribute to the rest [17]. Changing the energy carrier may not only significantly change the technical and operational features of the aircraft itself but also deeply transform the full air transport system (ATS), and even the energy production and supply system. Therefore, it is of utmost necessity to carry out environmental impact analysis even beyond the ATS level, including the energy supply e.g., nuclear, solar, wind, or biomass sources. The various possible combinations of energy supply and energy vector (battery, hydrogen, synthetic kerosene, etc.) make the evaluation of the energy consumption and climate impact of the future air transport system a challenging task. One major difficulty in reaching this objective is the complexity of the aircraft design process itself with a broad design space. Classical design processes present two kinds of limits. The first limitation is that they are defined to address kerosene powered aircraft [18–20]. The second limitation is that, even the

simplest tools proposed require geometrical and technological assessment as well as complex multidisciplinary analysis and optimization to evaluate one single aircraft configuration (MARILib, FAST-OAD, TASOPT [21]), [22–27]. The use of higher fidelity tools require the use of high computational capabilities and long design time.

In the following, a simple aircraft design procedure that covers various energy vectors is presented. From as small set of requirements in terms of capacity, range, storage medium, and propulsion system, the model allows one to retrieve the fuel (or energy) consumption for any mission.

This paper is organized as follows. In Section II, the minimal classical approach to designing aircraft and determining its main mass and operational features is discussed with its limitations in the context of the ecological transition of the ATS. Then, the models developed to address these limitations are proposed in Section III. Section IV proposed the validation of our model. Then, in Section V, the results of our model are proposed. Finally, Section VI proposed the conclusion of our work.

II. Minimal classical aircraft design approach

According to Breguet equation shown in (1), the performance of an aircraft in terms of fuel consumption (or energy), depends mainly on its characteristic weights (MTOW, OWE), its L/D in cruise, and its Specific Fuel Consumption (SFC).

$$Range = \frac{L/D \times \eta \times fhv}{g} \times \log\left(\frac{MTOW}{MTOW - MissionFuel}\right) \tag{1}$$

$$\implies MissionFuel = f_1(MTOW, Range, L/D, SFC, Speed) \tag{2}$$

The minimal classical approach for the computation of characteristic weights such as MTOW and OWE with a petrol propulsion system is based on the so-called mass-mission coupling process [18]. In the context of very early stages of the design process such as the conceptual design phase, the objective is to estimate the optimized MTOW of the aircraft that ensures both the necessary amount of structure and energy on board. This can be presented by the following optimization problem:

$$\begin{aligned} \min_{X \in \mathbb{R}^k} \quad & \text{MTOW} \\ \text{subject to} \quad & \text{structure and design mission fuel constraints} \end{aligned} \tag{3}$$

which is equivalent to solve

$$\begin{cases} MissionFuel = f_1(MTOW, Range, L/D, SFC, Speed), \\ MTOW = OWE + Payload + TotalFuel, \\ OWE = f_2(Geometry, MTOW, N_{pax}, Propulsion \quad system), \end{cases}$$

where f_1 is defined by (1). This approach does not need any geometry definition. However this model is based on empirical statistical regressions with classical tube and wing architectures:

$$\begin{cases} MissionFuel = f_1(MTOW, Range, L/D, SFC, Speed), \\ MTOW = OWE + Payload + \text{Total Fuel}, \end{cases}$$

where Total Fuel takes in account the mission fuel, reserve fuel, diversion and holding fuel.

$$\text{Total Fuel} = MissionFuel(1 + K_r) + \text{Diversion Fuel} + \text{Holding Fuel} \tag{4}$$

As shown in (5), the payload is computed with the number of passengers (N_{pax}) and a mass allowance (M_{pax}) presented in Table 1.

$$Payload = N_{pax} \times M_{pax}(Range) \tag{5}$$

In this classical minimum approach, the OWE can be divided into three parts.

$$OWE = Basic_{MWE} + OWE_{Payload} + OWE_{Propulsion} \tag{6}$$

where

Category	M_{pax} (kg/pax)	M_{fur} (kg/pax)
General	95	18
Commuter	105	18
Regional	110	22
Short-medium	115	22
Long-range	120	30

Table 1 Passenger mass allowance and furnishing mass.

- $OWE_{Payload}$ is the part of the OWE related to the furnishing and operator items. This quantity can be approximated as a function of N_{pax} and Range.
- $OWE_{Propulsion}$ is the part of the OWE related to the propulsion system. It depends on the type of the propulsion system and its maximum power. This last quantity will be approximated by the Generalized Power Index (GPI) defined in (10).
- $Basic_{MWE}$ is the part of the OWE that is independent of $OWE_{Propulsion}$ and $OWE_{Payload}$ in a conventional aircraft (structure and non-propulsive systems).

A. New propulsion systems

If the current kerosene-oriented propulsion system moves to electric propulsion with batteries or fuel cells and hydrogen tank, for instance, OWE computation in (6) should incorporate the weight of the battery or the weight of the fuel cell system and the hydrogen tank. The fuel cell system weight will be added to the propulsion weight as it depends on the installed power. The hydrogen tank or battery weights will be added to the equation as a new term:

$$OWE = Basic_{MWE} + OWE_{Payload} + OWE_{Propulsion} + OWE_{TankSystem} \tag{7}$$

$OWE_{TankSystem}$ is the OWE related to the tank system and depends on the type of fuel and the storage mode (e.g., compressed or liquefied gas). It is approximated as a function of the amount of fuel (or energy) to be stored and the type of storage system.

III. Models

This section deals with the regression models that allow us to determine the aircraft characteristics (such as MTOW and OWE) for different propulsion systems: thermal engines powered by the combustion of kerosene, hydrogen, or liquid methane or electric engines powered by batteries or a fuel cell system. First, the total mass of the structure and standard systems ($Basic_{MWE}$) that is required to build an aircraft is estimated for a given MTOW. Secondly, based on the ($Basic_{MWE}$), we rebuild the OWE of an aircraft that is powered by classical or new propulsion systems. Lastly, we determine MTOW.

A. Empty weight breakdown based on statistical regressions

In this part, a database of existing aircraft with classical design is used to derive a correlation between the MTOW and the manufacturer weight empty (or the total mass of structure and standard systems), noted $Basic_{MWE}$. $Basic_{MWE}$ is the part of OWE which is independent of $OWE_{Propulsion}$ and $OWE_{Payload}$ in the conventional aircraft, as expressed in (8). The aircraft database of about 227 passenger aircraft of all categories, from general aviation to long haul, is used to estimate $Basic_{MWE}$.

$$Basic_{MWE} = OWE - OWE_{Payload} - OWE_{Propulsion} \tag{8}$$

1. OWE related to payload

Operating weight empty related to payload, $OWE_{payload}$, is computed as follows:

$$OWE_{payload} = W_{furnishing} + W_{op_{items}} \tag{9}$$

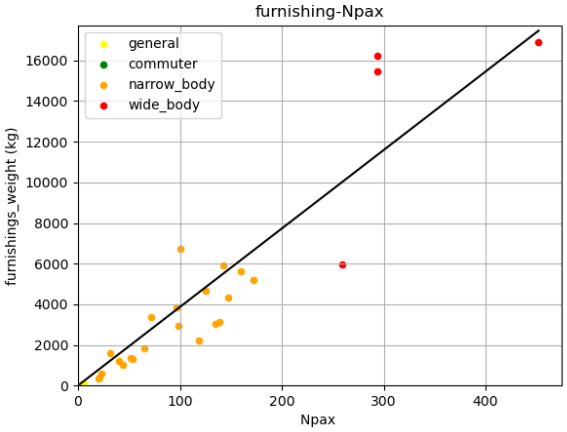

Fig. 1 Correlation between number of passenger and furnishing weight. Data from ref. [28, 29].

The weight of the furnishing, $W_{furnishing}$, is estimated by a linear regression model, which is shown in Fig. 1. The model is built using the 38 types of aircraft data collected from [28, 29].

In Fig. 1, we select a linear regression such that

$$W_{fur} = M_{fur}(Range) \times Npax,$$

where M_{fur} the furnishing mass budget per passenger. It is assumed to depend on the flight range as described in Table 1. For the estimation of operational items weight, we used the following function :

$$W_{op_{items}} = 5.e^{-6} \times Npax \times distance$$

The operational items represent the set of crew provisions, passenger cabin supplies, potable water and toilet chemicals, safety equipment, oil residual fuel, and cargo handling equipment [30].

2. OWE related to the propulsion system

The mass of the propulsion system components is assumed to depend on their "power". But the overall characteristics of turbofans (e.g., weight, dimensions, cost, etc.) are generally linked to their maximum thrust, which is most often quantified at low speed and low altitude. The Sea Level Static Thrust ($SLST$) is most often used to drive the engine as a whole (e.g., thrust, weight, size, etc.). Meanwhile, the characteristics of turboprops or reciprocating engines are generally linked to their maximum shaft power: $MaxPower$. To gain in generality, the Generalized Power Index (GPI) is defined. This quantity, expressed in the unit of power (Watts), is a figure of interest to estimate the weight of an engine, whatever its type. It is defined as follow:

$$GPI = \begin{cases} MaxPower & \text{engine with propeller,} \\ PW & \text{turbofan,} \end{cases} \tag{10}$$

where $MaxPower$ is the maximum shaft power of the turboprop or piston engine. To be consistent with all engine types, PW is created. It represents the maximum power of turbofan engine. This quantity is defined by equation (11).

$$PW = n_e \frac{SLST \times V_{2min}}{\eta_f}, \quad \text{where} \quad V_{2min} = \frac{V_{app} \times 1.13}{1.23}. \tag{11}$$

V_{2min} is the minimum takeoff speed and V_{app} is the approach speed. Both are defined as a function of the 1g stall speed, V_{s1g}, as follows.

$$V_{2min} = 1.13 \times V_{s1g} \quad \text{and} \quad V_{app} = 1.23 \times V_{s1g}$$

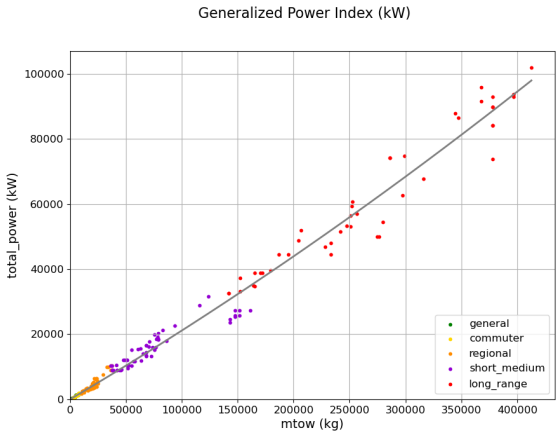

Fig. 2 Correlation between MTOW and GPI

The minimum takeoff condition, V_{2min} is the speed near sea-level at which the turbofan delivers its maximum thrust (SLST). It is computed from V_{app}, which is easily found in most aircraft databases. PW is representative of the shaft power delivered by the engine in takeoff conditions.

The total GPI (including all engines) is correlated to the $MTOW$ of all airplanes in the database. The graph Fig. 2 illustrates this correlation together with a second-order polynomial least square fit.

$$GPI = 8.31693845e^{-5} \times MTOW^2 + 2.03027049e^{2} \times MTOW - 1.05e^{5}$$

The mass of the propulsion system, $OWE_{propulsion}$ is then estimated using the gravimetric indices (GI), which are represented with a unit in kW/kg.

$$OWE_{propulsion} = W_{engine} + W_{thruster}, \quad \text{where} \quad W_{engine} = \frac{GPI}{GI_i} \quad \text{and} \quad W_{thruster} = \frac{GPI}{GI_{tj}}.$$

i represents the type of propulsion system, and j represents the type of thruster. The different gravimetric indices (GI) are computed as follows.

- $GI_{turbofan} = 4.3kW/kg$ (shown in Fig. 3) and $GI_{t_{fan}} = 15kW/kg$ for a turbofan engine
- $GI_{turboshaft} = 4.3kW/kg$ (shown inFig. 4) and $GI_{t_{propeller}} = 10kW/kg$ for a turboprop engine
- $GI_{piston} = 1.1kW/kg$ (shown in Fig. 5) and $GI_{t_{propeller}} = 10kW/kg$ for a piston engine

The GIs are computed by the regressions between dry weight and GPI, as shown in Figs. 3 to 5. The data used in these figures are from [29] for the current petrol-based propulsion systems and from manufacturers databases for new technologies.

3. Estimation of $Basic_{MWE}$

As shown in Fig. 6, the correlation between the OWE and the MTOW is very tight, regardless of the aircraft category. One possible explanation is that all these airplanes are designed to transport passengers, equipped with similar propulsion systems burning petrol derivatives (gasoline or kerosene). It can also be because the airplanes are designed using the same structural principles, and their designs are compliant with consistent regulation and economic pressure. Nevertheless, this regression that we observe includes two implicit links. The first one is between MTOW and the mass of the propulsion system and the second one is between OWE and payload. Different articles [31, 32] derive mass relationship only for hybrid and all-electric as well as fixed-wing and VTOL configurations. For each airplane of the database, we have estimated the $Basic_{MWE}$ as follows :

$$Basic_{MWE} = OWE - OWE_{payload}(Npax, Range) - OWE_{Propulsion}(GPI(MTOW)),$$

where $OWE_{payload}$, $OWE_{Propulsion}$ and GPI are computed as presented above in this chapter.

We found the following regression (Fig. 7):

$$Basic_{MWE} = -3.18952359e^{-7} \times MTOW^2 + 4.22840552e^{-1} \times MTOW - 30 \tag{12}$$

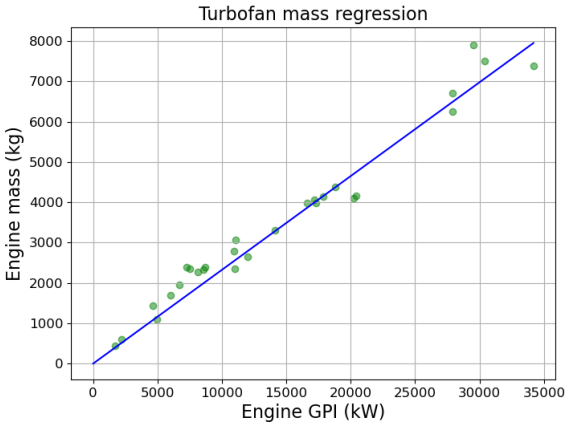

Fig. 3 Correlation between GPI and turbofan mass

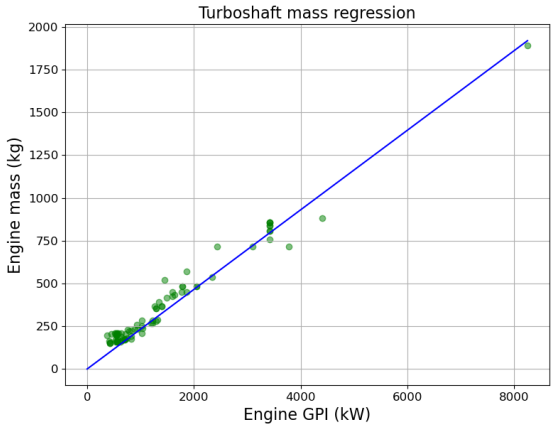

Fig. 4 Correlation between GPI and turboshaft mass

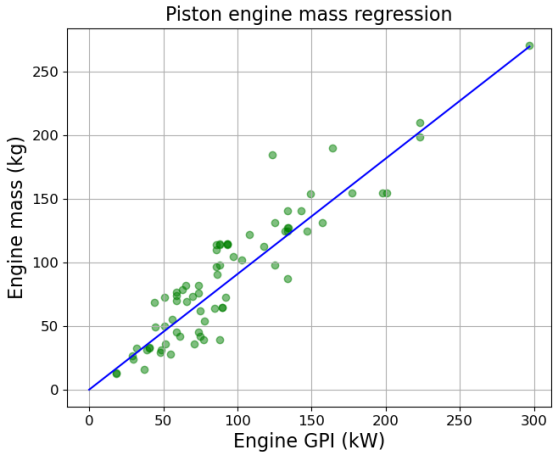

Fig. 5 Correlation between GPI and piston engine mass

Basic$_{MWE}$, which is computed as a function of MTOW, is independent of the number of passengers and of the propulsion system. We can use this quantity to estimate the OWE of airplanes with a non-petrol-based propulsion system and any passenger capacity. The freedom in the seating capacity is important because new propulsion technologies generally require putting additional on board systems compared to petrol-based architectures (e.g., liquid hydrogen tanks, fuel cells, etc.).

B. OWE related to electric and H2 propulsion

In Section III.A we already estimate $Basic_{MWE}$, $OWE_{Payload}$, $OWE_{propulsion}$. However, to compute OWE related to electric and H2 propulsion, $OWE_{propulsion}$ needs to be reevaluated for electric and hydrogen technologies.

1. All electric with batteries

The weight of the electric propulsion system can be defined as the set of electric motor weight and electronics system weight.

$$OWE = Basic_{MWE} + OWE_{payload} + OWE_{electricpropulsionsystem} \tag{13}$$

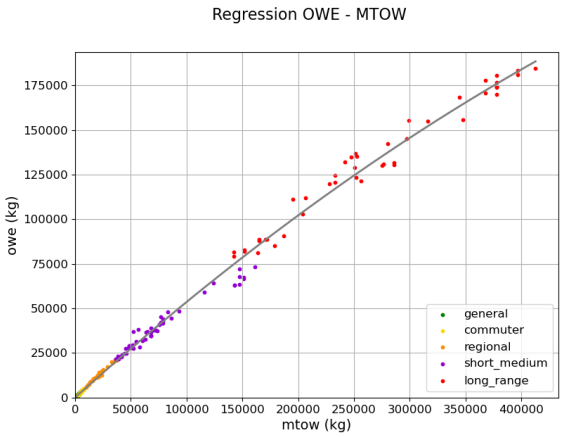

Fig. 6 Correlation between MTOW and OWE

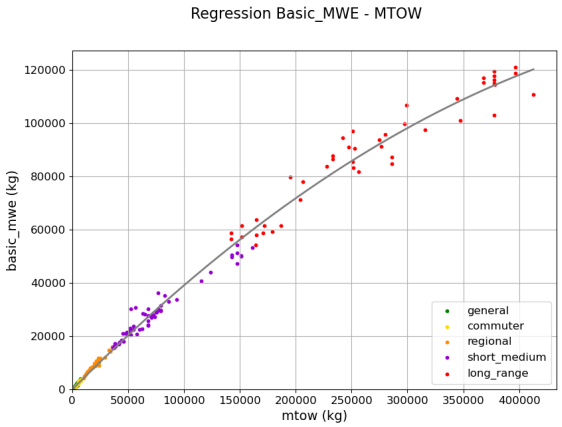

Fig. 7 Correlation between MTOW and $Basic_{MWE}$

For electric motors, we use the gravimetric index of Magnix 500 engine :

$$GI_{electric} = 4.1kW/kg^{*}$$

This value might be quite pessimistic since the Siemens SP260D engine have gravimetric index of $5.2kW/kg$ [33] and Kadyk *et al.* [34] forecasted that the gravimetric index of an electric motor airplane can reach up to $10kW/kg$ in the future. Additionally, we use the following values for the gravimetric index of power electronics.

$$GI_{power_{elec}} = 10kW/kg$$

In the estimation of $MTOW$, $Total fuel$ includes the battery weight estimated thanks to the energy density of battery.

2. hydrogen fuel cell aircraft

The weight of an electric propulsion system (motor + power electronics), $OWE_{electric\ propulsion\ system}$, computed using (13).

$$OWE = Basic_{MWE} + OWE_{payload} + OWE_{electric\ propulsion\ system} + OWE_{fuel_{cell}} + OWE_{Tanksystem}$$

The weight of the fuel cell system must include not only the fuel cell stack but also the balance of plant (e.g. compressor, valves, manifolds, air inlet, humidity regulator etc.) and cooling devices (heat exchanger). The gravimetric index for a fuel cell is as follows:

$$GI_{fuel_{cell}} = 1kW/kg$$

This value is twice higher than existing packaging tailored for trucks. For exemple, Horizon Fuel Cell Technologies [†] is selling liquid-cooled fuel cell systems of 120 kW with a power density of around 0.5 kW/kg. Meanwhile, the literature seems to be rather optimistic: Dudfield [35] cited a report which forecasts 1.6 kW/kg for drones applications (air-cooling) while Kadyk *et al.* [34] estimated that metallic bipolar plates (with adequate corrosion coating) would strongly reduce the stack weight, enabling $8kW/kg$ fuel cell systems in the future.

Tank system mass is related to the type of fuel and how it is packaged. At the granularity level of our models, gasoline or kerosene requires no special structures as they are stored in the existing structural parts. Hydrogen and methane require special devices and can be stored in compressed or liquefied form. The mass of the different tank types is defined using a gravimetric index [36] defined as follows:

$$G_{index} = \frac{M_{fuel}}{M_{fuel} + M_{tank}}$$

*https://cleantechnica.com/2019/10/24/750-horsepower-electric-aviation-engine-tested-by-magnix/

[†]www.horizonfuelcell.com, accessed on November 2023. VL II series liquid-cooled system.

For liquid hydrogen ($\sim 20K$), The company Hypoint clamed in 2022 to be able to build LH2 tanks with a gravimetric index of 0.5, which is quite challenging[‡]. A study on hydrogen storage explains that the gravimetric index of liquid hydrogen could reach 0.7 [37]. However, we take 0.4 to consider the possible difficulties in reaching the targeted value of 0.5. Considering that liquid methane is also cryogenic ($\sim 111K$) [38] and is a bit less challenging to store compared to liquid hydrogen, we take 0.8 as the gravimetric index.

Liquid methane can be obtained at ambient temperature with a pressure of about 10 bars. So, its cryogenic storage is not considered, and only compressed storage has been evaluated. The gravimetric index of the cryogenic storages is as follows:

$$\text{Liquid hydrogen} : G_{index_{LH_2}} = 0.4, \text{ according to [36]}$$
$$\text{Liquid methane} : G_{index_{LCH_4}} = 0.8, \text{ presented in Section .B}$$

The mass of pressurized vessels is computed according to the performance index expressed as follows:

$$P_{index} = \frac{P_i \times V_i}{M_{tank}}$$

The performance index depends on the level of tank's technology. According to the Sheet 4.2 of France-Hydrogene [§], the most efficient technology makes use of carbon fiber-reinforced plastic (CFRP) and have a performance index equal to 661 bar.L/kg. We take this value as a reference. Knowing the initial pressure of the gas into the tank, we can get the gravimetric index of the tank from the performance index:

$$G_{index_{gas}} = \frac{1}{1 + \frac{P_i}{P_{index} \times \rho_{gas}(P_i)}}$$

In the estimation of $MTOW$, we consider $Total fuel$ as the weight of liquid hydrogen or liquid methane.

3. Empty weight for hydrogen (methane) fuelled aircraft

$$OWE = Basic_{MWE} + OWE_{payload} + OWE_{propulsionsystem} + OWE_{Tanksystem}$$

Liquid hydrogen or liquid methane engine are supposed to have the same mass as the conventional engine. But their Specific Fuel Consumption (SFC) [23] is computed according to the fuel lower heating value (FHV) given in Table 2. The computing method of $OWE_{Tanksystem}$ is the same as those of hydrogen fuel cell airplanes.

Fuel	FHV (MJ/kg)
Kerosene	43.1
Hydrogene	121
Methane	50.3

Table 2 Fuel lower heating value used in this study.

C. Determination of MTOW

In the context of our models, optmizing MTOW is equivalent to solving the following system of two equations:

$$\begin{cases} MissionFuel = f_1(MTOW, Range, L/D, SFC, Speed) \\ MTOW = OWE + Payload + TotalFuel \end{cases} \tag{14}$$

where, OWE, Payload, and Total fuel are already defined. In order to increase the precision of the model, two additional relations are introduced.

[‡]https://hydrogen-central.com/hypoint-zero-emission-hydrogen-flight-range-ultralight-liquid-hydrogen-fuel-tanks/ accessed on November 2023
[§]https://www.france-hydrogene.org/fiches-techniques/ accessed November 2023.

	η
E-motors powered by fuel cells	$\eta_p \times \eta_{elec} \times \eta_{fcs}$
For reciprocating engines or turboprops	$\eta_h \times \eta_{pw}$
Turbofans	$\eta_{th} \times \eta_{pr}$
Battery-based energy storage	$\eta_p \times \eta_{elec}$

Table 3 Propulsion system efficiencies

- The first one relates SFC with GPI and the type of the propulsion systems :

$$SFC = f_9(GPI, PropulsionType), \tag{15}$$

  where f_9 is defined in Section .B.
- The second one relates L/D and the MTOW:

$$L/D = f_8(MTOW), \tag{16}$$

  where f_8 is a correlation based on Fig. 9.

1. Generalized Breguet equation

When fuel consumption is involved, we use the following Breguet equation, which can be easily reversed to compute Fuel:

$$Range = \frac{L/D \times \eta \times fhv}{g} \times \log\left(\frac{MTOW}{MTOW - MissionFuel}\right)$$

For battery-based energy storage, we use the following equation:

$$Range = \frac{L/D \times \eta \times bed}{g} \times \frac{M_{battery}}{MTOW}$$

As described in Table 3, the efficiency η refers to the whole propulsion chain, from tank (or battery) to propulsive power. For a conceptual airplane design approach, the following efficiencies are assumed to be constant :

- η_p is the thruster efficiency. it can be a propeller ($\eta_h = 0.80$) or a fan ($\eta_f = 0.82$) eventually driven by an electric motor.
- The electric motor efficiency with its power electronics: $\eta_{elec} = 0.95$
- The fuel cell system efficiency: $\eta_{fcs} = 0.5$

PSFC of typical light aircraft piston engines is in the range between 0.24kg/h/kW and 0.5kg/h/kW [39, 40]. So we take the following constant as the power related SFC of **petrol piston** engines :

$$PSFC_{piston} = 0.25 \quad kg/h/kW,$$

which leads to the following power efficiency:

$$\eta_{pw} = 0.335.$$

Power-related SFC of **petrol turboshafts** has been taken from a regression on a set of 83 different engines , which is presented in Fig. 8. The following formula is derived from the regression:

$$PSFC_{turboprop} = \left(5.54e^{-8} + \frac{2.77e^{-6}}{\left(\frac{GPI}{1000}\right)^{0.65}}\right),$$

which leads to the following power efficiency :

$$\eta_{pw} = \frac{0.084}{\left(0.2 + \frac{10}{\left(\frac{GPI}{1000}\right)^{0.65}}\right)}.$$

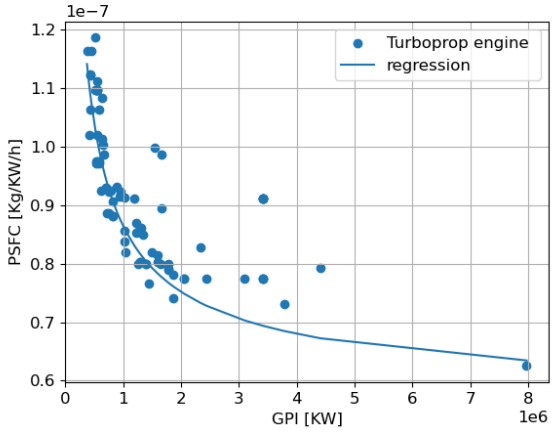

Fig. 8 Correlation between PSFC and GPI

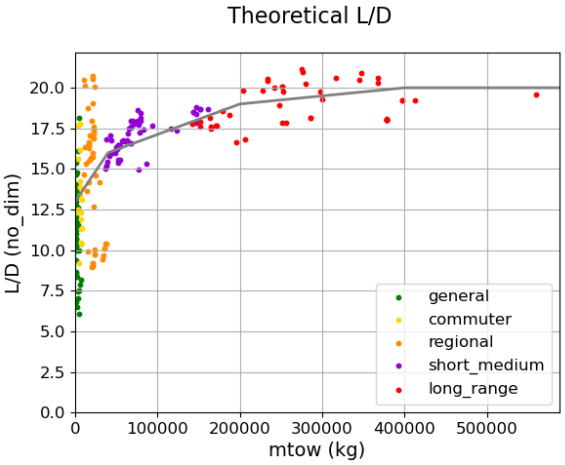

Fig. 9 lift-to-drag ratio estimated from geometry in the database (dots) and fit curve of Table 4 (black line).

The thrust-related SFC of petrol turbofans is computed using a constant η_{th} and a formula for η_{pr}. The formula is explained in Appendix Section VI.

$$\eta_{th} = 0.474, \qquad \eta_{pr} = \frac{1}{\frac{1}{2} + \sqrt{\frac{1}{4} + \frac{r \times \eta_{th} \times fhv}{2(1+BPR)V_0^2}}} \quad \text{with} \quad r = 0.02.$$

2. Approximation of the Lift to Drag Ratio

Lift to drag ratio L/D is linked to the geometry of the airplane : aspect ratio, airfoil, roughness ... etc. Fig. 9 shows L/D estimated from a few geometric parameters described in the database as a function of the MTOW. The L/D estimation method is described in [18, 41] and the code is available on the git repository [¶].

For large civil transport aircraft (short, medium to long range) the correlation between L/D and MTOW is rather satisfying : the L/D remains between 15 and 21, probably because all this airplanes have a very similar overall geometry. But for lighter airplanes, large discrepancies are observed. Despite this, an arbitrary L/D is chosen with respect to MTOW as specified in Table 4. The resulting trend is drawn (black-line) on Fig. 9

MTOW (kg)	0	40000	200000	500000	1000000
L/D	13	16	19	20	20

Table 4 Interpolation of lift-to-drag

At this stage, all the parameters of the system (14) are known, and it can be solved numerically.

IV. Validation

The validity of the model is assessed with kerosene airplanes. For other architectures, very few data are currently available. The model requires a design range and passenger capacity to return the characteristic weights (e.g., MTOW, OWE, MWE, etc.) and other parameters such as fuel burn for the design mission.

Fig. 10 (resp. 12) shows the estimated MTOW (resp. OWE) versus the real MTOW (resp. OWE). Fig. 11 (resp. 13) shows the relative error distribution $MTOW_{predicted} - MTOW/MTOW$ (resp. $OWE_{predicted} - OWE/OWE$.

The error distributions show that the model is able to predict MTOW and OWE with an accuracy equal or lower than 10% for 87% and 85% respectively of the aircraft in the database. For most airplanes the MTOW is predicted with less than 14% error.

[¶]https://gitlab.com/m6029/genericairplanemodel.git

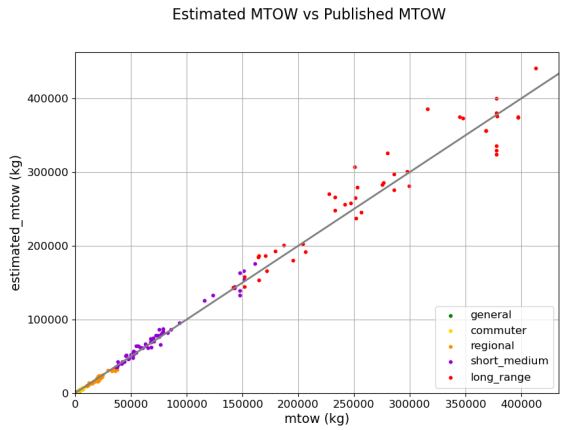

Fig. 10 Comparison between estimated MTOW and published MTOW

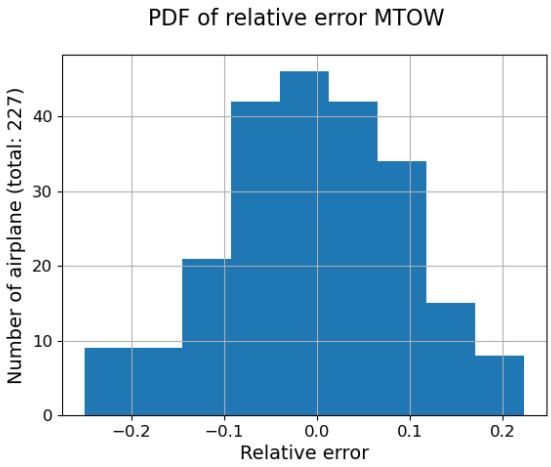

Fig. 11 Relative error distribution

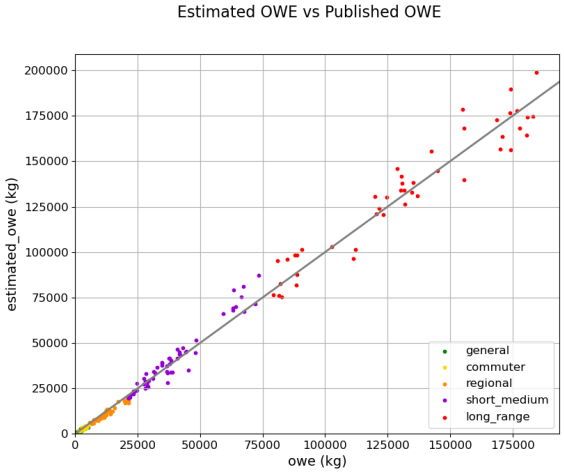

Fig. 12 Comparison between estimated MTOW and published MTOW

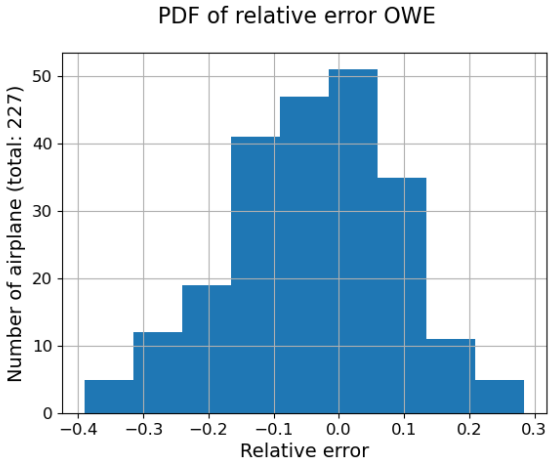

Fig. 13 Relative error distribution

Of course this model is not intended to make accurate predictions, but it provides orders of magnitude based on previously observed trends.

V. Results

A. Use case 1 : Assessment of the airplane Alice from EVIATION

Alice is probably the full electrical, battery-powered transport airplane with the highest performances among the recent projects. Its design has been evolving a lot since the beginning of the project, and currently, very few data are published by EVIATION. On its website[‖], we can find:

Making a full electric 9 passengers airplane flying over 460 km is very challenging, regarding the energy density of today's available batteries. To reach the required level of performance L/D and structural mass are probably MWE have probably been improved compared to conventional airplanes. But in which extend ?

The Generic Aircraft Model (GAM) can bring some elements to answer this question. In the model, both L/D and basic MWE (mainly structure + standard airplane systems) are coming from regressions over a full fleet of various

[‖] https://www.eviation.com/aircraft/ accessed on November 2023

Total length	Wing span	Cabin width	MTOW	Payload	Engine power	Maximum speed	Range[a]
$17.7m$	$19.2m$	$1.93m$	$8350kg$	$1130kg$	$2\times700Kw$	$480km/h$	$460km$

[a] with 30 mins reserve

Table 5 The specifications of Alice from EVIATION

classical aircraft. They represent some sort of medium technological level. But Alice is clearly out of this. EVIATION engineers have most probably adopted several strategies to compensate for the huge battery weight. Increasing L/D can be obtained by increasing wing aspect ratio and smoothing all wetted surfaces. Reducing MWE can be made thanks to a wide use of CFRP together with clever structural optimization and system selection.

In the GAM model, the cruise L/D can be set directly. An improvement factor of the MWE can be added. Consequently, we have two unknowns to figure out. In the following we add a design constraint : the claimed MTOW of 8350 kg is most probably ceiled by the maximum weight allowed for CS23 certification which is 8600 kg, with a margin of 250 kg. If we consider a MTOW of 8350 kg as a target for the design, this new constraint gives a relationship between the required L/D and the improvement factor on MWE. The resultinf compromise is shown on Fig. 14.

To perform this calculation, the cruise speed has been set to 380 km/h and we fixed the passenger mass allowance to reach the given payload with 9 passengers on board. Let's note that one can change any of the parameters to match his own context. The resulting graph is presented in Fig. 14 for three values of the battery energy density.

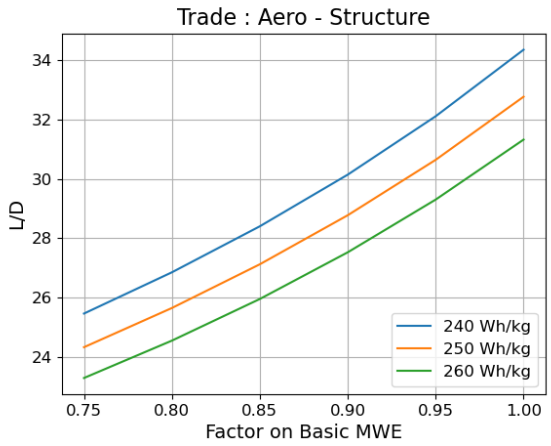

Fig. 14 Trade : Aero-Structure

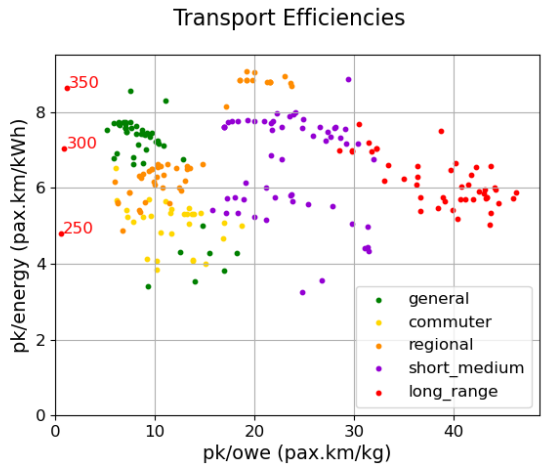

Fig. 15 Transport efficiencies

We can see that a 15% gain on the basic MWE requires an L/D of about 27, which is challenging for a commuter aircraft but achievable. A rapid analysis with the aerodynamic polar estimation method presented in [18, 41] leads to an L/D of about 27.9. In the following analysis, we consider a 15% gain on the basic MWE and an L/D of 27 for the Alice airplane.

In the future, the required energy and the amount of materials is likely to become a major driver of sustainability. The required amount of materials and energy to offer an airborne transport service can be put in perspective to the PK product of a specific airplane design (the nominal number of passengers times the design travel distance). We can form two indicators: PK/E and PK/OWE, which can be respectively interpreted as the energetic efficiency and the structural efficiency of a given airplane flying a given route.

According to these criteria, we can compare the efficiencies of Alice with other aircraft. Fig. 15 presents the position of Alice regarding these efficiencies, for three different values of the battery energy density (250, 300, and 350 Wh/kg).

The analysis is based on the nominal mission of each airplane to compute PK/E. The total energy stored in the kerosene for petrol airplane is set to 43.1 MJ/kg in our analysis .

Fig. 15 is interesting because it clearly shows the tendencies of these efficiencies regarding the different categories

of airplanes. We can see that Alice is competing with petrol commuters regarding energetic efficiency but is far less efficient regarding material efficiency. The physical characteristics of the battery-based electric power chain are responsible for that. We can also see that an energy density of 350 Wh/kg would push the airplane to the top level of energetic efficiency without entering the cloud for material efficiency. Of course, the use of PK/OWE as an indicator of material efficiency does not consider the type of material, which is critical when it comes to the batteries. However, our analysis, at least, gives an overview concerning the total amount of materials regardless of their types.

We also investigate how the PK/E evolves if we move the Capacity vs Range for Alice design. Fig. 16 displays this evolution of PK/E. The yellow frontier corresponds to MTOW limit of 8600 kg related to CS23 certification.

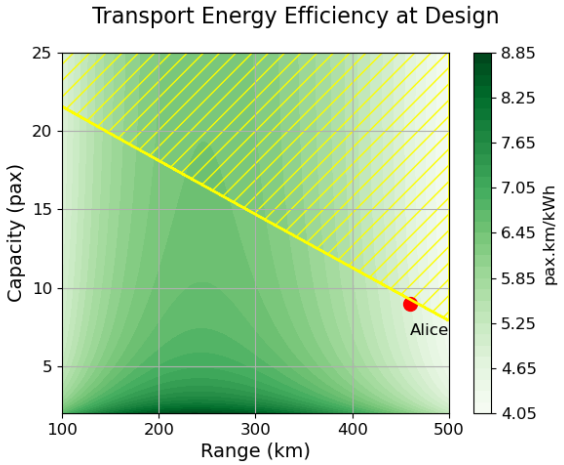

Fig. 16 Transport energy efficiency at Design

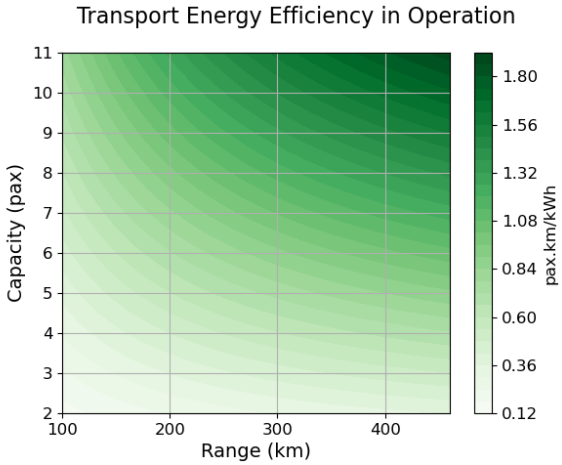

Fig. 17 Transport energy efficiency in Operation

An interesting element of Fig. 16 is the existence of an optimum range related to the energetic efficiency. The optimum range lies on about 250 km for a capacity of 9 passengers and slightly increases with the capacity. This implies that EVIATION company put priority on the maximum possible range. The existence of this optimum can be explained as follows. For ranges lower than the optimal one, the PK product increases more rapidly than the required mission energy, while the required mission energy increases more rapidly than the PK product for ranges higher than the optimal one.

Let's keep in mind this optimum range corresponds to the design mission (each point in Figure xxx corresponds to a different aircraft, designed with the related capacity and range). If we consider now Alice in an of design context, the evolution of mission PK/E is driven by on-board passengers and range as shown in Fig. 17.

Fig. 18 displays this evolution of PK/OWE by varying capacity and range.

Interestingly, the evolution of design mission PK/OWE also reveals an optimum range about 320 km, which is longer than that of PK/E. This optimum has the same trend as the optimum range from the PK/E. For ranges lower than the optimal one, the PK product increases more rapidly than the required empty weight, while the required empty weight increases more rapidly than the PK product for ranges higher than the optimal one.

Fig. 19 displays this frontier for a capacity of 9 passengers. To be consistent with the classic representation of the Pareto front where PK/E and PK/OWE are supposed to be independently minimized, we take the inverse of previous indicators, which are represented as E/Pk and OWE/PK in the figure.

According to the Pareto front, a good compromise between energetic and material efficiency could be at about 300 km for the design range. The anchor point for material efficiency at 320 km, however, would not be a bad choice as it makes the corresponding range a relevant indicator for the global efficiency of the design.

If now, we consider the range that optimizes the material efficiency PK/OWE, we can compute the evolution of this maximum when the battery energy density varies. Fig. 20 shows, in green color, the variation of the best range while varying the energy density of the battery. Blue lines refer to the optimum range if we accept a variation of ±10% around the optimal PK/OWE.

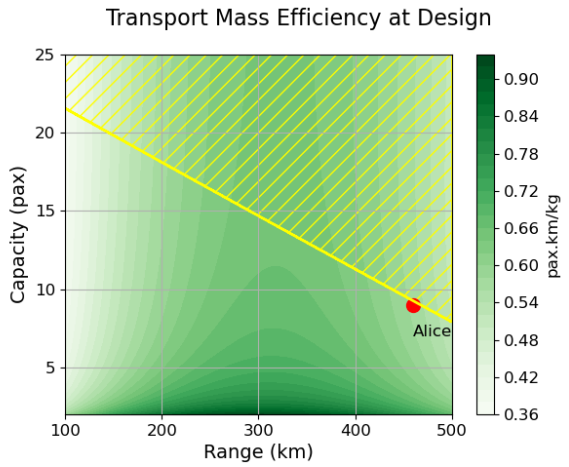

Fig. 18 Transport energy efficiency at Design

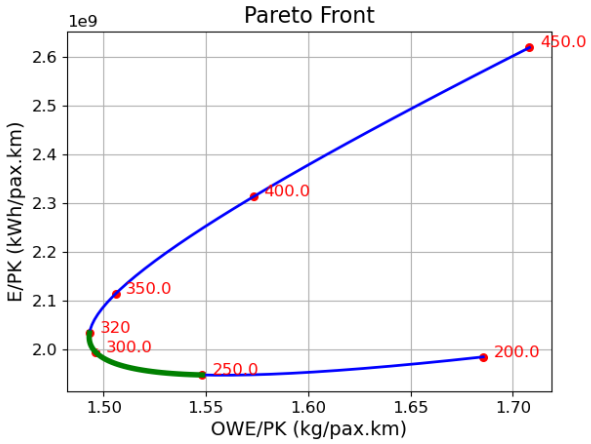

Fig. 19 Pareto Front

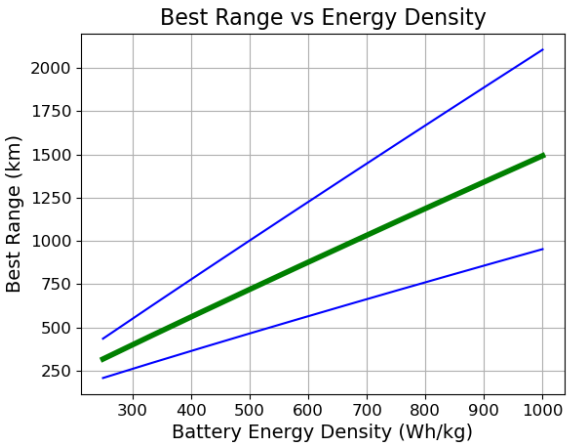

Fig. 20 Best range vs Energy density

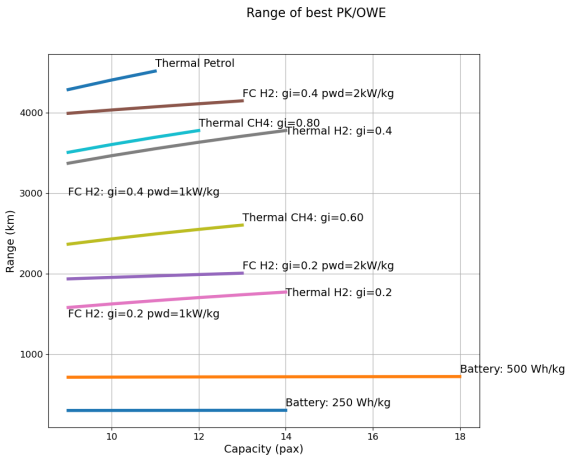

Fig. 21 Range of best PK/OWE

We can see that , ranges approximately between 750 and 1000 km would be achievable with an energy density of about 400 Wh/kg, which is claimed to be reachable within a decade [citation].

As shown in the presentation of GAM model, an Alice airplane model can be set up as follows:

Power system	Design mission
energy type : battery	category : commuter
engine count :2	payload : 9
engine type : emotor	speed : 380 km/h
thruster type : propeller	range : 460 km
bpr : None	altitude : 3048 m

Table 6 Step 1: Characteristic of Alice airplane

This study illustrates a possible application of the GAM model to identify some main characteristics of an aircraft from limited initial information. Here, we focuse on a full electric commuter from EVIATION, and we evaluate the required level of lift to drag ration, L/D, and structural alleviation that allow to fly with 9 passengers over the maximum

Specific data
maximum fuel factor (max fuel factor) : 1
battery energy density (battery enrg density) : 250Wh/kg
stdm factor: 0.84
lift-to-drag (lod) : 27

Table 7 Step 2 : Add specific data to the Alice airplane

Distance	460 km
Take Off Weight	8350 kg
Payload	1125 kg
Total energy	862 kWh
Mission energy	638 kWh
Reserve energy	224 kWh

Table 8 Results of Alice model considering the characteristics in Table 6 and Table 7

possible range (460 km) according to the maximum take off weight allowed in CS23.

B. Use case 2

Potential propulsion technologies for a 19-passenger commuter are listed as follows:

1) Electric motor with battery
2) Electric motor with hydrogen fuel cell
3) Turboshaft burning hydrogen
4) Turboshaft burning methane
5) Turboshaft burning kerosene

Except for turboshaft burning kerosene, which is considered mature, all other propulsion technologies present at least one critical characteristic that would require some improvements listed as follows:

- Battery energy density (currently ≈ 250 Wh/kg)
- 1000 V barrier for electric motor (currently ≈ 700 to 800 V limiting the power to ≈ 1 to 2 MW)
- Fuel cell efficiency (currently ≈ 50% to 60% max resulting in huge heat power to dissipate)
- Fuel cell overall power density (currently ≈ 1kW/kg due to a huge balance of plant)
- Gravimetric index of liquid hydrogen & methane tanks (currently respectively ≈ 0.1 and 0.2)
- Cryogenic fuel management (20K for liquid hydrogen and 111K for liquid methane)

The most important evolution in the near future will be on the battery energy density, fuel cell power density, and cryogenic tanks' gravimetric index.

Some companies (like HyPoint) are claiming that they can produce tanks with the gravimetric index of 0.5 (without a balance of plant), and a lot of research have been undertaken to reach a battery energy density of about 500 Wh/kg [42]. Concerning fuel cell integration, a more compact balance of plant should bring significant improvement of fuel cell energy density at system level.

The GAM model allows a quick assessment of the possible benefit in terms of airplane performances from the evolutions of technological efficiencies. Our focus is on CS23 commuters (capacity lower or equal to 19 passengers). We first look for the maximum capacity that can be obtained at the range that maximizes the criterion PK/OWE. For this study, we apply the same technological improvements that we found from the Alice airplane (L/D = 27, Basic$_{MWE}$ factor = 0.85) to the battery airplanes. For all other airplanes, we let the standard estimations performed by the model, e.g. L/D from regression as presented in Section III.C.2 , and mass aleviation factor = 1. These assumptions implies that airplane shapes and aerodynamic cleanliness are more driven by the manufacturing and production costs of classical metallic structures, which can be seen as a bit conservative.

As mentionned in the use case I presented in Section V.A, we considered the optimum range according to PK/OWE as an indicator of the efficiency of a given technology. Fig. 21 shows these optimal ranges together with the maximum possible passenger capacity (MTOW limited at 8600kg), for different values of battery energy densities and cryogenic tank gravimetric index. It is noted that a gravimetric index of 0.2 for hydrogen corresponds to 0.6 for methane and 0.4 for hydrogen corresponds to 0.8 for methane. We can get at least four interesting insights from the figure, which are listed as follows:

- Good performance of battery-powered airplanes regarding the maximum passenger capacity, provided the energy density of batteries can be pushed to 500 Wh/kg. This is due to the improvement in L/D and MWE versus other technologies.
- Impossibility for state of the art fuel cell airplanes to fly 19 passengers, even if the tank gravimetric index reaches its highest value.
- Except for battery-powered airplanes, all other technologies reveal optimal ranges higher or equal to 1500 km.

Let's keep in mind that the presented ranges are the ones that optimize the PK/OWE of each propulsive technology. All types of airplanes can be designed for shorter ranges, but with lower PK/OWE. Table 9 gives the main figures for the different concepts, and Fig. 22 illustrates the maximum ranges.

	Name	Range	L/D	Eff	OWE	MTOW	PK/OWE	PK/E
1	Battery: 250 Wh/kg	185	27.5	0.72	6605	8600	0.53	5.62
2	Battery: 500 Wh/kg	694	27.5	0.72	6605	8600	2	10.74
4	FC H2: gi=0.4 pwd=1kW/kg	122	13.63	0.36	6548	8600	0.35	1.36
5	FC H2: gi=0.2 pwd=2kW/kg	1093	13.63	0.36	6412	8600	3.24	3.31
6	FC H2: gi=0.4 pwd=2kW/kg	2192	13.63	0.36	6260	8600	6.65	3.66
7	Thermal H2: gi=0.2	1388	13.63	0.2	6205	8600	4.25	1.99
8	Thermal H2: gi=0.4	2859	13.63	0.2	5861	8600	9.27	2.19
9	Thermal CH4: gi=0.60	1839	13.63	0.2	5433	8600	6.43	2.16
10	Thermal CH4: gi=0.80	2509	13.63	0.2	5091	8600	9.36	2.28
11	Thermal Petrol	2745	13.63	0.2	4733	8600	11.02	2.35

Table 9 Aircraft characteristics for fixed MTOW

Let's note that the efficiency (Eff) in the table corresponds to the ratio of propulsive power (Thrust . Speed) over primary power (Fuel flow . Fuel Heating Value or power sucked from the battery).

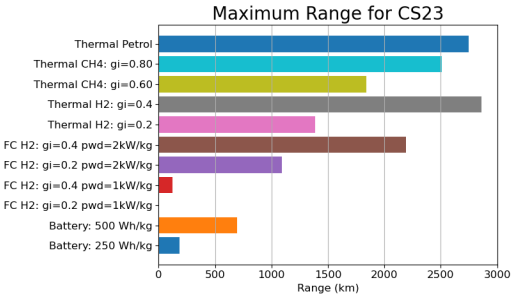

Fig. 22 Maximum range for CS23

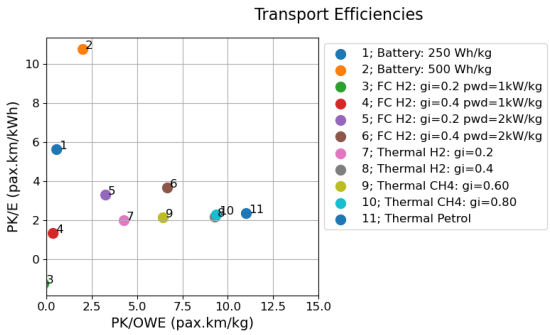

Fig. 23 Transport efficiencies

- We observe that state of the art battery (250 Wh/kg) airplanes are not able to produce a significant range.
- Similarly, none of the state of art fuel cell configurations (power density $\approx$ 1 kW/kg), even with a highly efficient tank (gi=0.4) is able to fly longer than 2800 km.
- If we put apart state of the art battery and fuel cell, all other technology types and maturity levels can fly a 1000 km range with 19 passengers.

- When fuel cell energy density reaches about 2 kW/kg, hydrogen fuel cell-powered airplanes are showing similar ranges as turboprop burning hydrogen.
- We observe the very good performance of hydrogen-fueled thermal technology, which shows a potential even higher than petrol, provided the tank gravimetric could reach about 0.4 kg of H2 per kg of H2+tank.
- We also observe the very good performance of methane-powered airplanes, even with a tank gravimetric of about 0.6 kg of CH4 per kg of CH4+tank (which corresponds to 0.2 for hydrogen).

If we plot all these concepts in a graph PK/OWE – PK/E, we obtain Fig. 23. We observe that:

- Reaching a cryogenic tank gravimetric index of about 0.4 for hydrogen and 0.8 for methane would put these technologies at the same level of efficiency as petrol.
- Both TGI of 0.4 or power density of 2 kW/kg are not able, individually, to unlock the fuel cell technology. If combined, these evolutions could push the fuel cell technology to a high level of energetic efficiency and a certain level of material efficiency.
- According to PK/E, the high efficiency of battery airplanes is partially due to the L/D and MWE improvements. If those improvements were applied to other propulsive technologies than full electric, they would bring improvements as well.

Fig. 24 shows the transport efficiencies of the studied configurations in comparison with those coming from the airplanes in the data base.

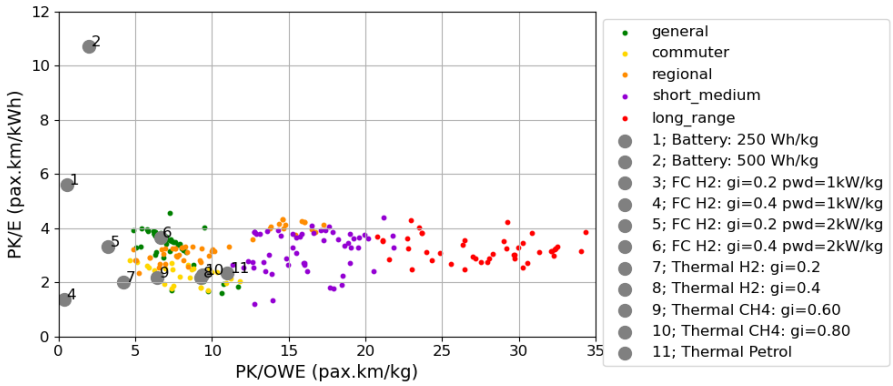

Fig. 24 Transport efficiencies vs database

We observe that:

- The energetic efficiency of battery airplanes (1 and 2), enhanced by structural and aerodynamic improvements, are far above the cloud of point, whatever the aircraft category.
- A global gravimetric energy density of fuel cell systems of about 2 kW/kg pushes the fuel cell-powered airplanes on top of the cloud of points (5 and 6).
- Only thermal configurations with highly efficient tanks (8 and 9) are able to compete with the material efficiency of petrol-powered airplanes.

Main characteristics of airplanes designed for a nominal range of 1000 km (when possible) are presented in Table 10.

- Battery airplanes as well as state of the art fuels cell concepts are not able to reach the required distance. An energy density of 500 Wh/kg is able to provide a range.
- Material efficiency (PK/OWE) is reduced due to the range decrease in comparison to the values in Table 9

The presented study gives some inside view into the potential, in terms of range and capacity, of different propulsion technologies in the commuter segment. Studied propulsion systems were:

1) Electric motor with battery
2) Electric motor with hydrogen fuel cell
3) Turboshaft burning hydrogen
4) Turboshaft burning methane
5) Turboshaft burning kerosene

The study gives a global overview of the different technologies according to energy efficiency (PK/E), material efficiency (PK/OWE), maximum capacity, and maximum range. It enlightened the high potential of fuel cell-powered airplanes

	name	range	L/D	Eff	OWE	MTOW	PK/OWE	PK/E
1	Battery: 250 Wh/kg	185	27.5	0.72	6605	8600	0.53	5.62
2	Battery: 500 Wh/kg	694	27.5	0.72	6605	8600	2	10.74
4	FC H2: gi=0.4 pwd=1kW/kg	122	13.63	0.36	6548	8600	0.35	1.36
5	FC H2: gi=0.2 pwd=2kW/kg	1000	13.61	0.36	6170	8340	3.08	3.35
6	FC H2: gi=0.4 pwd=2kW/kg	1000	13.51	0.36	4878	7021	3.9	3.95
7	Thermal H2: gi=0.2	1000	13.54	0.19	5032	7301	3.78	2.11
8	Thermal H2: gi=0.4	1000	13.42	0.18	3544	5773	5.36	2.46
9	Thermal CH4: gi=0.60	1000	13.48	0.19	3987	6580	4.77	2.32
10	Thermal CH4: gi=0.80	1000	13.44	0.18	3447	6004	5.51	2.47
11	Thermal Petrol	1000	13.43	0.18	3248	5885	5.85	2.52

Table 10 Aircraft characteristic for fixed range (when it is possible)

provided the required level of maturity for fuel cell power density and cryogenic tanks gravimetric index. The study has shown the interest of methane-powered airplanes, provided this methane is coming from renewable sources.

C. Hydrogen powered airplane efficiency

A crucial question for hydrogen as an aviation fuel is the range capability of hydrogen-powered airplanes in comparison to petrol-based one. Two aspects of the hydrogen technology are particularly critical:

- The weight of the tank (not the weight of fuel)
- The required volume to store the fuel

In this study, the proposed model can represent the tank weight, but not its volume. Still, it can give a trend of the hydrogen airplane energetic efficiency. This parameter is measured by PK/E, passenger-kilometer per fuel energy reacquired for the design mission.

First a reference kerosene aircraft is defined:

Power system	Design mission
energy type : kerosene	category : long range
engine count :2	payload : 350
engine type : turbofan	speed : 875 km/h
thruster type : fan	range : 14000 km
bpr : 12.5	altitude : 35000 ft

Table 11 Requirements for the reference long-range keresosene aircraft.

Then, with the same set of requirements, the energy type is set to liquid hydrogen. The design range is varied from 4000 km to 14000 km. In all cases, the gravimetric index of liquid hydrogen tanks (TGI) has also been varied from 0.4 to 0.7, but the actual gravimetric index is more likely equal to 0.2 [43]. According to the company HyPoint, 0.4 (including the balance of plant) is already a challenging value. 0.7 appears in some theoretical publications as a feasible proposition for an entry into service in 12-15 years [44]. The results are shown on Fig. 25.

- The PK/OWE criterion seems to split the global fleet into three domains:
  - General, commuter and some regional airplanes, below 10 pax.km/kg (green, yellow and orange dots)
  - Short and medium range airplanes, between 10 and 20 pax.km/kg (purple dots)
  - Long range airplanes, beyond 20 pax.km/kg (red dots)
- For a Tank Gravimetric Index equals to 0.4 (TGI =0.4), liquid hydrogen-powered airplanes can not escape from the short-medium range domain.
- The range of optimal PK/OWE evolves from about 7000km (for TGI=0.4) to about 14000km (for TGI=0.7). Additionally, we found that a TGI higher than 0.5 is necessary to penetrate into the efficiency domain of long range kerosene aircraft.

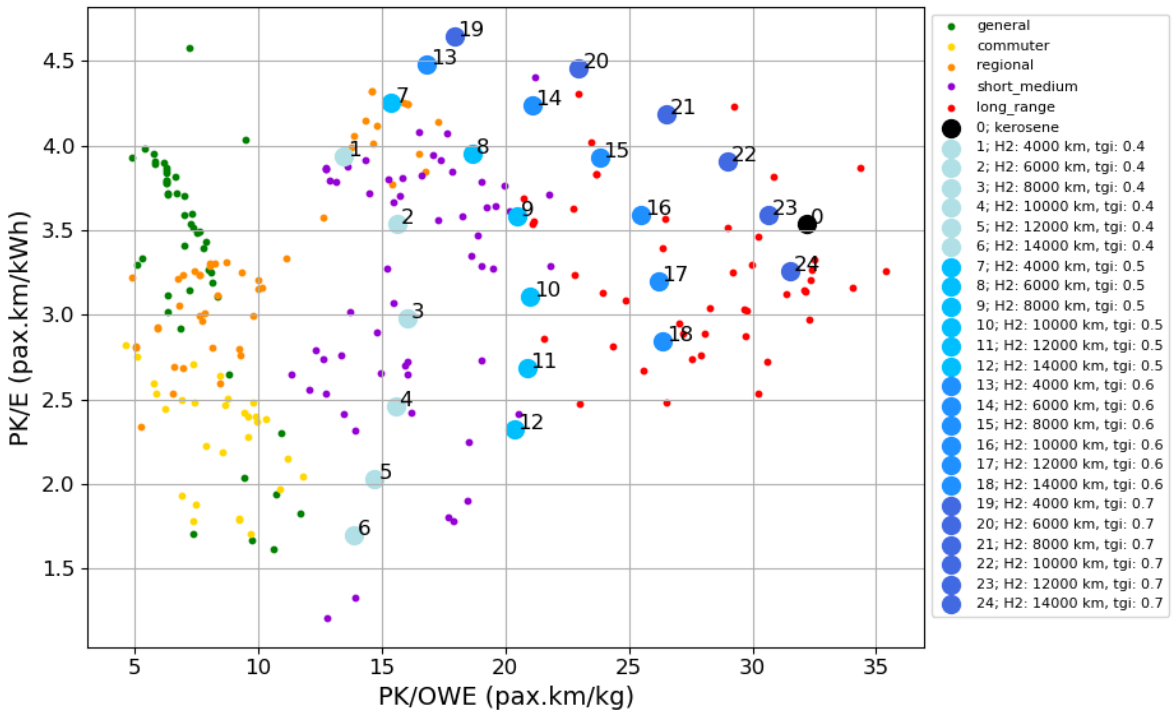

Fig. 25 Transport efficiencies map. Small dots stand for for kerosene aircraft in the database. Large blue dots stand for an aircraft with a liquid-hydrogen tank, with different gravimetric index and design range.

- At TGI of 0.7 would put the hydrogen airplane in a very good position in the efficiency domain, better than most of the existing long ranger.

Even very simple model presented in this study can reveal an already-known result about the domain of applicability of hydrogen-based thermal propulsion. This result gives additional evidence of the applicability of our model.

VI. Conclusion

This paper introduced a simple and very fast model of airplane design and operation. This model allows one to capture some important characteristics of an airplane, such as design weights, range, capacity, speed, fuel, or energy consumption, without the need to define the geometry of the aircraft. The model can simulate various propulsive technologies based on electric motors, batteries, fuel cells, or thermal engines burning kerosene, methane, or hydrogen. The global technological indices proposed in this work enable modeling such propulsion technologies with easy adjustment towards the technical evolution or forecasts. Three possible applications have been presented. The first one allows the identification of the technical challenges in the Alice airplane from the company called EVIATION. The second one has presented an overview of the transport potential, in terms of range and passenger capacity, of different propulsive technologies applied to the 19-passenger, CS23, commuter segments. The last application allows one to identify the technological limit of thermal hydrogen-powered airplanes in relation to the maturity of the components of the propulsive system. All the models are available open source according to the CeCILL-C Free Software License Agreement on a git repository[**]

[**]https://gitlab.com/m6029/genericairplanemodel.git commit number cc5683feff706f483e3632171feda4ad0df8edfc

Appendix A

A. Nomenclature

V_{cs} = Core engine exhaust Speed
V_{fs} = Fan exhaust speed
$\dot{m}_c$ = Core air mass flow rate
$\dot{m}_f$ = Fan air mass flow rate
$\dot{m}_a$ = Total air mass flow rate

B. Demonstration

The following derivation is used in Section .B for turbofan engines. First, the thrust F is expressed as a function of the exhaust speeds in the engine core and engine fan ? Kinetic power $\mathcal{P}_{cin}$.

$$F = \dot{m}_c(V_{cs} - V_0) + \dot{m}_f(V_{fs} - V_0) \tag{A.B.1}$$

$$= \dot{m}_a\left(\frac{\dot{m}_c V_{cs} + \dot{m}_f V_{fs}}{\dot{m}_a} - V_0\right) \tag{A.B.2}$$

$$F = \dot{m}_a(V_j - V_0) \quad \text{with} \quad V_j = \frac{\dot{m}_c V_{cs} + \dot{m}_f V_{fs}}{\dot{m}_a} \tag{A.B.3}$$

$$\mathcal{P}_{cin} = \frac{1}{2}\dot{m}_c(V_{cs}^2 - V_0^2) + \frac{1}{2}\dot{m}_f(V_{fs}^2 - V_0^2)$$

$$\mathcal{P}_{cin} = \frac{1}{2}\dot{m}_a\left(\sqrt{\left(\frac{\dot{m}_c V_{cs}^2 + \dot{m}_f V_{fs}^2}{\dot{m}_a}\right)^2} - V_0^2\right)$$

$$\mathcal{P}_{cin} = \frac{1}{2}\dot{m}_a(V_{j'}^2 - V_0^2) \quad \text{avec} \quad V_{j'} = \sqrt{\left(\frac{\dot{m}_c V_{cs}^2 + \dot{m}_f V_{fs}^2}{\dot{m}_a}\right)}$$

The relative error between V_j and $V_{j'}$ is evaluated using the difference between V_j and $V_{j'}$, as presented as follows.

$$V_{j'}^2 - V_j^2 = \frac{\dot{m}_c V_{cs}^2 + \dot{m}_f V_{fs}^2}{\dot{m}_a} - \left(\frac{\dot{m}_c V_{cs} + \dot{m}_f V_{fs}}{\dot{m}_a}\right)^2$$

$$= \frac{\dot{m}_c \dot{m}_f (V_{cs} - V_{fs})^2}{\dot{m}_a^2}$$

Hence, the relative error between V_j and $V_{j'}$ is expressed as follows.

$$\frac{V_{j'}^2 - V_j^2}{V_j^2} = \frac{\dot{m}_c \dot{m}_f (V_{cs} - V_{fs})^2}{(\dot{m}_c V_{cs} + \dot{m}_f V_{fs})^2} \simeq 14\% \tag{A.B.4}$$

For the rest of the demonstration, we consider $V_j^2 = V_{j'}^2$ with a relative error of 14%, as shown in (A.B.4).

Appendix B

To demonstrate that $\eta_{pr} = \dfrac{1}{\frac{1}{2}+\sqrt{\frac{1}{4}+\dfrac{\alpha\eta_t f hv}{2V_0^2(1+bpr)}}}$, consider $\mathcal{P}_{cin} = \frac{1}{2}\dot{m}_a(V_j^2 - V_0^2)$ with V_j defined as in (A.B.1).

$$\dot{m}_a = \dot{m}_c + \dot{m}_f \tag{B.1}$$

$$bpr = \frac{\dot{m}_f}{\dot{m}_c} \tag{B.2}$$

$$\dot{m} = \alpha\dot{m}_c \tag{B.3}$$

$$\text{(B.1)\&(B.2)} \implies \dot{m}_a = \dot{m}_c(1+bpr) \tag{B.4}$$

$$\text{(B.3)\&(B.4)} \implies \dot{m}_a = \frac{\dot{m}}{\alpha}(1+bpr) \tag{B.5}$$

$$F = \dot{m}_a \delta V \quad \text{with} \quad \delta V = V_j - V_0 \tag{B.6}$$

$$\eta_{pr} = \frac{FV_0}{\mathcal{P}_{cin}} = \frac{\dot{m}_a \delta V \times V_0}{\frac{1}{2}\dot{m}_a(V_j^2 - V_0^2)} = \frac{1}{1+\frac{\delta V}{2V_0}} \quad \text{with} \quad V_j \quad \text{defined in} \quad \text{(A.B.1)} \tag{B.7}$$

$$SFC = \frac{\dot{m}}{F} \tag{B.8}$$

$$SFC = \frac{V_0}{\eta_t \eta_{pr} f hv} \tag{B.9}$$

$$\text{(B.7)\&(B.9)} \implies SFC = \frac{2V_0 + \delta V}{2\eta_t f hv} \tag{B.10}$$

$$\text{(B.5)\&(B.6)} \implies F = \frac{\dot{m}}{\alpha}(1+bpr)\delta V \tag{B.11}$$

$$\text{(B.8)\&(B.11)} \implies \delta V = \frac{\alpha}{SFC(1+bpr)} \tag{B.12}$$

$$\text{(B.10)\&(B.11)} \implies 2\eta_t FHV \times SFC = 2V_0 + \frac{\alpha}{SFC(1+bpr)} \tag{B.13}$$

Finally, we have

$$\text{(B.13)} \iff 2\eta_t(1+bpr) f hv \times SFC^2 - 2V_0 SFC(1+bpr) - \alpha = 0 \tag{B.14}$$

$$SFC^2 - \frac{V_0}{\eta_t f hv} SFC - \frac{\alpha}{2\eta_t f hv(1+bpr)} = 0 \tag{B.15}$$

By solving the second-degree polynomial in (B.15), we get :

$$SFC = \frac{V_0}{\eta_t f hv}\left[\frac{1}{2} + \sqrt{\frac{1}{4} + \frac{\eta_t f hv \alpha}{2V_0^2(1+bpr)}}\right] \tag{B.16}$$

Knowing that (B.16) is equal to (B.9), we have

$$\eta_{pr} = \frac{1}{\frac{1}{2} + \sqrt{\frac{1}{4} + \dfrac{\eta_t f hv \alpha}{2V_0^2(1+bpr)}}}.$$

Appendix C

In the following we assume that

- the technologies for the cryogenic tank of liquid hydrogen and liquid methane are the same.
- the stored volume of fuel (liquid methane or hydrogen) is the same.

The gravimetric indices of liquid hydrogen and liquid methane, $G_{index_{LH2}}$ and $G_{index_{LCH_4}}$ are expressed as follows.

$$G_{index_{LH2}} = \frac{M_{LH2}}{M_{LH2} + M_{tank_{LH2}}} \quad \text{and} \quad G_{index_{LCH_4}} = \frac{M_{LCH_4}}{M_{LCH_4} + M_{tank_{LCH_4}}}$$

For a given volume of fuel, and for a given cryogenic tank technology, the above equations can be rearranged as follows.

$$\frac{M_{LH2}}{\rho_{LH2}} = \frac{M_{LCH_4}}{\rho_{LCH_4}} \implies \frac{M_{LH2}}{M_{LCH_4}} = \frac{\rho_{LH2}}{\rho_{LCH_4}} \quad \text{and} \quad M_{tank_{LCH_4}} = M_{tank_{LH2}} = M_t$$

$$G_{index_{LH2}} = \frac{1}{1 + \frac{M_t}{M_{LH2}}} \implies \frac{M_t}{M_{LH2}} = \frac{1}{G_{index_{LH2}}} - 1 \tag{C.1}$$

$$G_{index_{LCH_4}} = \frac{1}{1 + \frac{M_t}{M_{LCH_4}}} \implies \frac{M_t}{M_{LCH_4}} = \frac{1}{G_{index_{LCH_4}}} - 1 \tag{C.2}$$

If we divide (C.2) by (C.1), we obtain the following expression.

$$\frac{M_{LH2}}{M_{LCH_4}} = \frac{\frac{1}{G_{index_{LCH_4}}} - 1}{\frac{1}{G_{index_{LH2}}} - 1} = \frac{\rho_{LH2}}{\rho_{LCH_4}} \implies G_{index_{LCH_4}} = \frac{1}{1 + \left(\frac{1}{G_{index_{LH2}}} - 1\right)\frac{\rho_{LH2}}{\rho_{LCH_4}}}$$

References

[1] Terrenoire, E., Hauglustaine, D. A., Cohen, Y., Cozic, A., Valorso, R., Lefèvre, F., and Matthes, S., "Impact of present and future aircraft NO_x and aerosol emissions on atmospheric composition and associated direct radiative forcing of climate," *Atmospheric Chemistry and Physics*, Vol. 22, No. 18, 2022, pp. 11987–12023. https://doi.org/10.5194/acp-22-11987-2022, URL https://acp.copernicus.org/articles/22/11987/2022/.

[2] Snijders, T., and Melkert, J., "Effect of cruise altitude and alternative aviation fuels on radiative forcing," 2011. https://doi.org/10.2514/6.2011-5632.

[3] Lee, D., Fahey, D., Skowron, A., Allen, M., Burkhardt, U., Chen, Q., Doherty, S., Freeman, S., Forster, P., Fuglestvedt, J., Gettelman, A., Rodriguez De Leon, R., Lim, L., Lund, M., Millar, R., Owen, B., Penner, J., Pitari, G., Prather, M., and Wilcox, L., "The contribution of global aviation to anthropogenic climate forcing for 2000 to 2018," *Atmospheric environment (Oxford, England : 1994)*, Vol. 244, 2020, p. 117834. https://doi.org/10.1016/j.atmosenv.2020.117834.

[4] Boucher, O., Borella, A., Gasser, T., and Hauglustaine, D., "On the contribution of global aviation to the CO2 radiative forcing of climate," *Atmospheric Environment*, Vol. 267, 2021, p. 118762. https://doi.org/10.1016/j.atmosenv.2021.118762.

[5] Gao, H., et al., "Aircraft cruise phase altitude optimization considering contrail avoidance," Ph.D. thesis, Massachusetts Institute of Technology, 2013.

[6] Dallara, E., and Kroo, I., "Aircraft design: Trading cost and climate mpact," 2009. https://doi.org/10.2514/6.2009-1261.

[7] Bauen, A., Harris, A., Sim, C., Gudde, N., Prussi, M., and Scarlat, N., "CORSIA lower carbon aviation fuels: An assessment of the greenhouse gas emission reduction potential," *Applied Sciences*, Vol. 12, No. 22, 2022, p. 11818. https://doi.org/10.3390/app122211818, URL https://www.mdpi.com/2076-3417/12/22/11818.

[8] Seber, G., Escobar, N., Valin, H., and Malina, R., "Uncertainty in life cycle greenhouse gas emissions of sustainable aviation fuels from vegetable oils," *Renewable and Sustainable Energy Reviews*, Vol. 170, 2022, p. 112945. https://doi.org/10.1016/j.rser.2022.112945, URL https://linkinghub.elsevier.com/retrieve/pii/S1364032122008267.

[9] Planès, T., "Du dimensionnement de systèmes et d'architectures en conception avion à la simulation de scénarios prospectifs durables pour le transport aérien," Ph.D. thesis, Institut supérieur de l'aéronautique et de l'espace, France, december 2022.

[10] Pavlenko, N., and Searle, S., "Assessing the sustainability implications of alternative aviation fuels," *The International Council on Clean Transportation*, 2021.

[11] Cabrera, E., and de Sousa, J. M. M., "Use of Sustainable Fuels in Aviation—A Review," *Energies*, 2022. URL https://api.semanticscholar.org/CorpusID:247758190.

[12] Marszałek, N., and Lis, T., "The future of sustainable aviation fuels," *Combustion Engines*, 2022. https://doi.org/10.19206/CE-146696, URL http://www.combustion-engines.eu/The-future-of-sustainable-aviation-fuels,146696,0,2.html.

[13] Chiaramonti, D., "Sustainable Aviation Fuels: the challenge of decarbonization," *Energy Procedia*, Vol. 158, 2019, pp. 1202–1207. https://doi.org/10.1016/j.egypro.2019.01.308, URL https://linkinghub.elsevier.com/retrieve/pii/S1876610219303285.

[14] Yusaf, T., Fernandes, L., Abu Talib, A. R., Altarazi, Y. S. M., Alrefae, W., Kadirgama, K., Ramasamy, D., Jayasuriya, A., Brown, G., Mamat, R., Dhahad, H. A., Benedict, F., and Laimon, M., "Sustainable aviation—yydrogen is the future," *Sustainability*, Vol. 14, No. 1, 2022-01-05, p. 548. https://doi.org/10.3390/su14010548, URL https://www.mdpi.com/2071-1050/14/1/548.

[15] ICAO, "Introduction to the ICAO basket of measures to mitigate climate change," 2007.

[16] Planès, T., Delbecq, S., Pommier-Budinger, V., and Bénard, E., "Simulation and evaluation of sustainable climate trajectories for aviation," *Journal of Environmental Management*, Vol. 295, 2021, p. 113079. https://doi.org/10.1016/j.jenvman.2021.113079, URL https://hal.science/hal-03325405.

[17] ATAG, "Waypoint 2050," , 2021. URL https://aviationbenefits.org/media/167417/w2050_v2021_27sept_full.pdf.

[18] Raymer, D., *Aircraft Design: A Conceptual Approach, Sixth Edition*, 2018. https://doi.org/10.2514/4.104909.

[19] Sadraey, M. H., *Aircraft design : A system engineering approach*, Aerospace series, Wiley, Chichester, 2013.

[20] Gudmundsson, S., *General Aviation Aircraft Design: Applied Methods and Procedures*, Elsevier Science & Technology, San Diego, 2022.

[21] Drela, M., "TASOPT 2.00: Transport aircraft system optimization—Technical description," , 2010.

[22] Yuhara, T., Makino, Y., and Rinoie, K., "Conceptual design study on liquid hydrogen-fueled supersonic transport considering environmental impacts," *Journal of Aircraft*, Vol. 53, No. 4, 2016, pp. 1168–1173. https://doi.org/10.2514/1.C033369, URL https://doi.org/10.2514/1.C033369.

[23] Oak, M., Fabre, A., Delavenne, M., Van, E. N., Benard, E., and Defoort, S., "Spectral project - Application of FAST-OAD code to the conceptual design of a hydrogen fuelled commercial aircraft," *IOP Conference Series: Materials Science and Engineering*, Vol. 1226, No. 1, 2022, p. 012027. https://doi.org/10.1088/1757-899X/1226/1/012027, URL https://iopscience.iop.org/article/10.1088/1757-899X/1226/1/012027.

[24] Maciel Monjon, M. M., and Monzu Freire, C., "Conceptual design and operating costs evaluation of a 19-seat all-electric aircraft for regional aviation," *2020 AIAA/IEEE Electric Aircraft Technologies Symposium (EATS)*, 2020, pp. 1–16.

[25] Yang, B., Lou, F., and Key, N. L., "Conceptual design of a 10-passenger thin-haul electric aircraft," *2020 AIAA/IEEE Electric Aircraft Technologies Symposium (EATS)*, 2020, pp. 1–18.

[26] Nam, G.-D., Vuong, L. D., Sung, H.-J., Lee, S. J., and Park, M., "Conceptual design of an aviation propulsion system using hydrogen fuel cell and superconducting motor," *IEEE Transactions on Applied Superconductivity*, Vol. 31, No. 5, 2021, pp. 1–7. https://doi.org/10.1109/TASC.2021.3064526, conference Name: IEEE Transactions on Applied Superconductivity.

[27] Nicolay, S., Karpuk, S., Liu, Y., and Elham, A., "Conceptual design and optimization of a general aviation aircraft with fuel cells and hydrogen," *International Journal of Hydrogen Energy*, Vol. 46, No. 64, 2021, pp. 32676–32694. https://doi.org/10.1016/j.ijhydene.2021.07.127, URL https://linkinghub.elsevier.com/retrieve/pii/S0360319921027920.

[28] Wild, T. W., *Aircraft powerplants*, 8th ed., McGraw-Hill, New York, 2014.

[29] Roux, E., *Avions civils à réaction Plan 3 vues et donneées caractéristiques*, Editions Elodie Roux, Blagnac, 2007.

[30] Torenbeek, .-., Egbert, *Synthesis of subsonic airplane design : an introduction to the preliminary design of subsonic general aviation and transport aircraft, with emphasis on layout, aerodynamic design, propulsion and performance*, Delft University Press Martinus Nijhoff Publishers, Delft, 1988.

[31] Hu, J., and Booker, J., "Preliminary sizing of electric-propulsion powertrains for concept aircraft designs," *Designs*, Vol. 6, 2022, p. 94. https://doi.org/10.3390/designs6050094.

[32] Riboldi, C., and Gualdoni, F., "An integrated approach to the preliminary weight sizing of small electric aircraft," *Aerospace Science and Technology*, Vol. 58, 2016, pp. 134–149. https://doi.org/10.1016/j.ast.2016.07.014, URL https://linkinghub.elsevier.com/retrieve/pii/S1270963816303601.

[33] Siemens, "Rekord-Motor SP260D und Extra 330LE," *Technical report*, 2017.

[34] Kadyk, T., Winnefeld, C., Hanke-Rauschenbach, R., and Krewer, U., "Analysis and Design of Fuel Cell Systems for Aviation," *Energies*, 2018. https://doi.org/10.3390/en11020375.

[35] Dudfield, C., "Beyond Batteries: Hydrogen Fuel Cells for UAVs," *Technical report*, 2016.

[36] Druot, T. Y., Peteilh, N., Roches, P., and Monrolin, N., "Hydrogen Powered Airplanes, an exploration of possible architectures leveraging boundary layer ingestion and hybridization," *AIAA SCITECH 2022 Forum*, American Institute of Aeronautics and Astronautics, San Diego, CA & Virtual, 2022. https://doi.org/10.2514/6.2022-1025, URL https://arc.aiaa.org/doi/10.2514/6.2022-1025.

[37] Joaquim R. R. A. Martins, "Hydrogen-Powered Aircraft: Concepts, Technologies, and Environmental Impact," , Mar. 2023. https://doi.org/10.52843/cassyni.5p1tcg, URL https://doi.org/10.52843/cassyni.5p1tcg, journal Abbreviation: Brahmal Vasudevan Institute for Sustainable Aviation Seminar Series Publication Title: Brahmal Vasudevan Institute for Sustainable Aviation Seminar Series.

[38] Dorrington, G., "Conceptual design of sustainable liquid methane fuelled passenger aircraft," 2013. https://doi.org/10.3233/978-1-61499-302-5-391.

[39] Senzig, D., and Liu, S., "Rotorcraft performance data for AEDT," 2016. https://doi.org/10.13140/RG.2.2.30060.97920, URL http://rgdoi.net/10.13140/RG.2.2.30060.97920, publisher: Unpublished.

[40] Kumar, T., Mohsin, R., Majid, Z. A., Ghafir, M. F. A., Yusuf, N. K., Kim, J., Wash, A. M., and Sahri, D. M., "Response surface methodology application in optimization of performance and exhaust emissions of RON 98, aviation gasoline 100LL and the blends in Lycoming O-320 engine," *Fuel*, Vol. 256, 2019, p. 115909. https://doi.org/10.1016/j.fuel.2019.115909, URL https://linkinghub.elsevier.com/retrieve/pii/S001623611931261X.

[41] Rebuffet, P., *Aérodynamique expérimentale : Cours professé à l'Ecole Nationale Supérieure de l'Aéronautique. Tome II*, 1966.

[42] Hepperle, M., "Electric Flight - Potential and Limitations," 2012. URL https://api.semanticscholar.org/CorpusID:35409144.

[43] Xisto, C., and Lundbladh, A., "Design and performance of liquid hydrogen fuelled aircraft for year 2050 EIS," *In 33rd congress of International council of the aeronautical sciences*, 2022.

[44] Huete, J., Nalianda, D., and Pilidis, P., "Impact of tank gravimetric efficiency on propulsion system integration for a first-generation hydrogen civil airliner," *The Aeronautical Journal*, Vol. 126, No. 1302, 2022, p. 1324–1332. https://doi.org/10.1017/aer.2022.60.